Grating-enhanced second-harmonic generation in polymer waveguides: role of losses

E. Popov, M. Neviere, R. Reinisch, J.-L. Coutaz, and J. F. Roux

A numerical study of second-harmonic (SH) generation in a corrugated polymer waveguide is performed with a rigorous electromagnetic theory. Comparison with experiment reveals the role of losses inside the waveguide—small losses do not significantly affect the nonresonant response and reduce the resonant enhancement of SH generation. High losses can lead to the opposite effect—instead of enhancement, dips in the SH efficiency are observed in the vicinity of guided-wave excitation. The peculiarities of the angular dependencies of SH generation are explained from the phenomenological point of view, and the role of phase matching is discussed.

1. Introduction

Optical waveguides made from organic polymers have attracted a great deal of interest in the past few years.[1] It is expected that similar devices will perform many useful functions in optical signal processing,[2,3] such as light modulation, second-harmonic (SH) generation, and optical logic. The guiding geometry is chosen because of its capability of concentrating energy.[4,5] Organic polymers are preferred because of their higher second-order susceptibility $\chi^{(2)}$ (Refs. 6–8) and better transparency in the visible and the near-infrared regions. Their nonlinear (NL) properties seem to change by less than 10% over a duration of 5 years, they can endure high-power laser beams (up to 1 GW/cm^2), and they can be easily spin coated. The most promising materials are at present obtained by copolymerization of a monomer (styrene, MMA, or urethane). There are hopes to generate green and blue light by doubling the frequency of near-infrared-emitting diodes by the use of the NL properties of these layers and enhancement of the light density through excitation of guided waves. The technical and economical consequences of succeeding in this aim are obvious and explain the efforts made in many laboratories.

Our contribution follows the experimental research previously done by Kull *et al.*[9] on a corrugated waveguide made of spin-coated polyurethane on a silver grating. The spectroscopic study of the influence of resonances on the SH generation reveal several unexpected features: Two pump wavelengths λ_1 were chosen in such a way that the signal wavelength ($\lambda_1/2$) falls either outside ($\lambda_1 = 1.319$ μm, $\lambda_1/2 = 0.6595$ μm) or inside ($\lambda_1 = 1.064$ μm, $\lambda_1/2 = 0.532$ μm) the absorption band of polyurethane. When the angle of incidence is properly chosen, a waveguide mode or a plasmon surface wave can be excited, resulting in an increase of the electric field at the pump frequency inside the NL guiding layer. Thus an enhancement of the SH generation is expected under these circumstances. Indeed, such enhancement was observed with a pump wavelength equal to 1.319 μm, but for the other pump wavelength (1.064 μm), minima were observed instead of maxima at the SH frequency. To the best of our knowledge, until now this behavior was unexplained.

It is the aim of this paper to show that a resonance phenomenon can lead either to an increase or to a decrease of the SH efficiency, depending on the losses at the SH frequency, the key point being the existence of complex zeros of the scattered diffraction order amplitudes.[10] Several different approaches have been

E. Popov and M. Neviere are with the Faculté des Sciences et Technique de St. Jérôme, Laboratoire d'Optique Electromagnétique, Unité Recerche Associee au Centre Nationale de la Recerche Scientifique 843, 13397 Marseille Cedex 20 France. E. Popov is also with the Institute of Solid State Physics, 72 Tzarigrasko Chaussee, 1784 Sofia, Bulgaria. R. Reinisch and J. F. Roux are with the Laboratoire d'Electromagnétisme, Microondes et Optoélectronique, Unité Recherche Associee au Centre National de la Recherche Scientique 833. ENSERG, 23 Avenue des Martyrs, Batiment 257, 38016 Grenoble Cedex, France. J.-L. Coutaz is with the Laboratoire d'Hyperfréquences et de Caractérisation, Université de Savoie, Campus Scientifique, F-73 376 Le Bourget du Luc, France.

Received 9 June 1994; revised manuscript received 20 December 1994.

0003-6935/95/183398-08$06.00/0.

recently proposed to deal theoretically with NL interaction in optical waveguides with phase or surface relief gratings,[11–14] and we choose a rigorous electromagnetic theory[15] based on Maxwell's equations, with the only assumption being the undepleted pump approximation.

2. Comparison of Linear and Nonlinear Responses Given by Theory and Experiment

The device investigated experimentally in Ref. 9 is described schematically in Fig. 1. It consists of a spin-coated layer (index n_2 and thickness t_2) on a silver grating (optical index n_3, grating period d, and groove depth h), illuminated by TM-polarized light with a circular frequency ω_1 at an angle of incidence θ_i. Because of the NL properties of the layer the diffracted light has two components at ω_1 and ω_2. The polymer crystallographic group is $C_{\infty mm}$, and it has an absorption edge of 630 nm.

The main difficulty in comparing theoretical and experimental results arises from the fact that both the grating and the material parameters are never known. Whereas in the investigation of nonresonant linear or NL response this uncertainty can lead to only a small error, the resonant phenomena are quite sensitive to variation of layer thickness, losses, groove depth, etc. The period can be measured most easily, and it is taken to be equal to 1.66 μm. Talystep measurements determine the groove depth of 80 nm. Layer thickness is equal to 3.0 ± 0.1 μm. The real parts of the refractive indices can be determined more or less precisely from the positions of the anomalies. The determination of absorption losses that was done by measurement of the propagation length of the guided waves contains greater uncertainty, and that is why we present results for several values of the losses expressed by the imaginary part of the optical indices. The first case with pump frequency 1.319 μm is called the low-losses case, and the second (1.064-μm pump frequency) is called the high-losses case. In the first (low-losses) case two different values of losses are investigated to show their influence on the SH response. For clarity we reproduce here the experimental figures from Ref. 9 (Figs. 2 and 4) at the pump and the SH frequencies. The comparison of experimental with numerical results can be done directly with Figs. 3 and 5.

In fact simple comparison of the experimental and the numerical results does not yield an explanation of the difference between the high- and the low-losses cases. We just substitute one black box (the experimental one) with another (the numerical code). To have a satisfactory physical explanation, one must look deeper into the mechanisms that govern the device response. Fortunately, rigorous theory can serve as a microscope with variable magnification. It provides for the possibility of varying all the system parameters precisely enough to separate their influence on the entire device response, turning the experimentalists' dreams into reality.

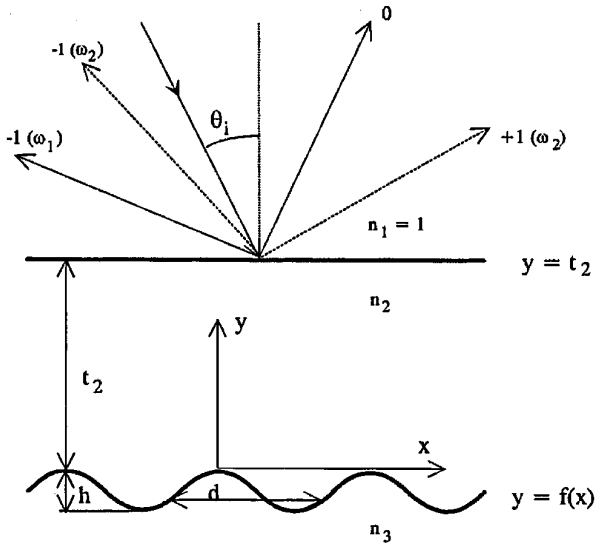

Fig. 1. Schematic representation of the corrugated NL waveguide.

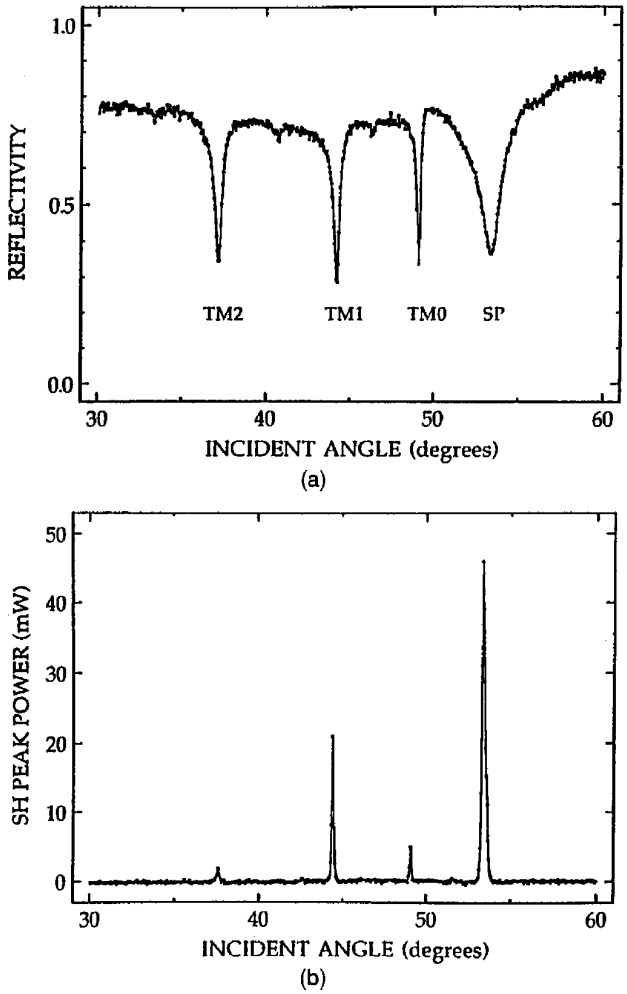

Fig. 2. (a) Experimental linear reflectivity at wavelength 1.319 μm. (See figure 2 of Ref. 9.) (b) Experimental SH peak power detected in the specular reflectance as a function of the angle of incidence. The pump wavelength is 1.319 μm, and the pump power is 40 kW. (See figure 4 of Ref. 9.)

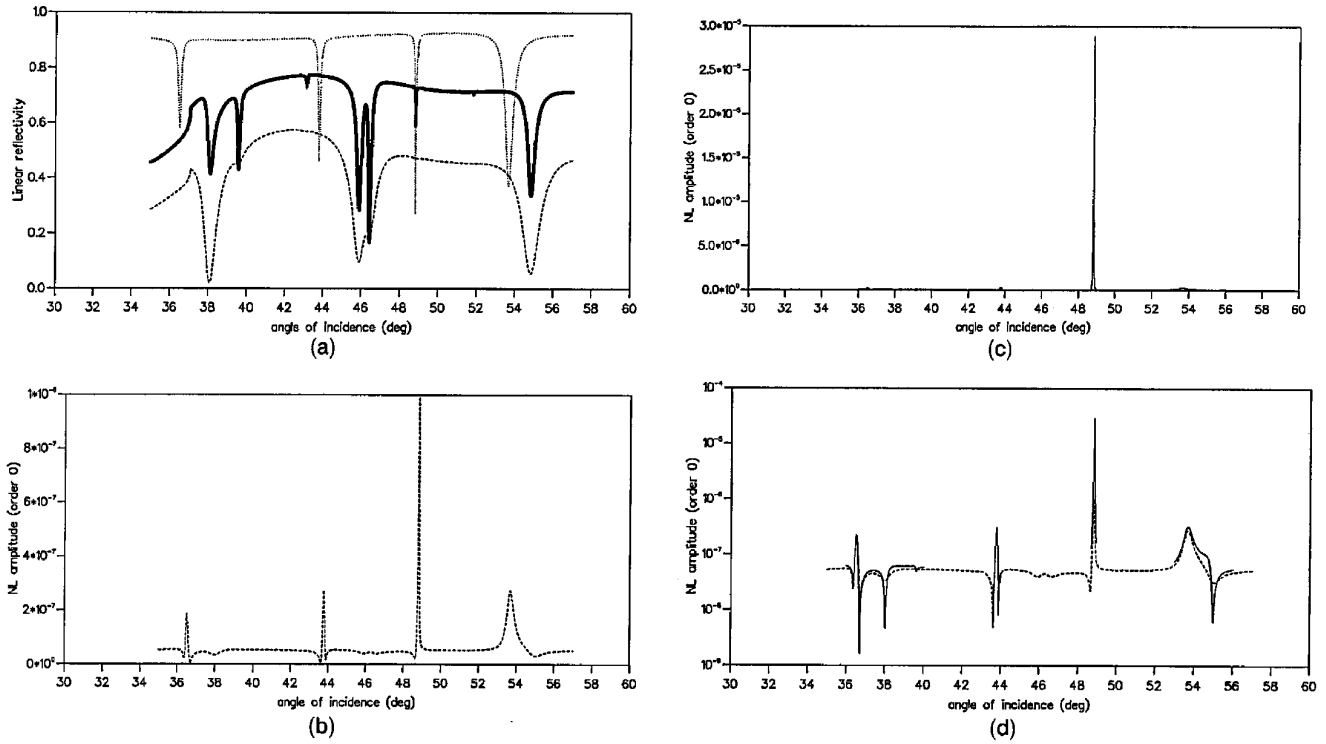

Fig. 3. (a) Angular dependence of the linear reflectivity. The dotted curve is at wavelength 1.319 μm, with $n_2(\omega_1) = 1.57 + i0.00004$, $n_3(\omega_1) = 0.05976 + i8.3668$. The other two curves are at wavelength 0.6595 μm: dashed curve, $n_2(\omega_2) = 1.585 + i0.0027$, $n_3(\omega_2) = 0.09363 + i3.5361$; solid curve, $n_2(\omega_2) = 1.585 + i0.000027$, $n_3(\omega_2) = 0.06363 + i3.5361$. The groove period is 1.66 μm, the groove depth is 0.08 μm, and the thickness is 2.92 μm. Numerical results are for TM polarization. (b) NL specular amplitude at 0.6595 μm. The refractive indices correspond to the dashed curve in Fig. 3(a). (c) NL specular amplitude at 0.6595 μm. The refractive indices correspond to the solid curve in Fig. 3(a). (d) same as in Figs. 3(b) and 3(c), but on a semilogarithmic scale.

There is no doubt that the anomalies in the SH angular behavior are connected with resonances, i.e., guided waves (waveguide modes and plasmon surface waves) in the device. However, we have to distinguish between two main mechanisms of birth of peaks or dips:

(I) Incident light is coupled through the grating periodicity to a guided wave at the same optical frequency. Then, in general, there is an enhancement of the optical energy density inside the waveguide (when the waveguide mode is excited) or near the metal–dielectric interface, when a plasman surface wave is generated. When squared, this enhanced field inside the NL layer could lead to much stronger SH generation than what is observed far away from the resonances.

(II) The second mechanism involves one more resonance: the guided wave of ω_1 excites a guided wave at ω_2. It is believed that the resulting double (in fact it is a triple one—the first resonance at ω_1 is squared) resonance (phase matching between the modes at ω_1 and ω_2) would lead to stronger SH generation.

Indeed, a comparison between the linear reflectivity and the SH response in the low-losses case indicates that when a guided wave is excited, there is a dip in the linear reflectivity and a peak in the SH specular amplitude. Unfortunately this idyllic intuitive picture is completely spoiled when one looks at the high-losses case: instead of peaks, there are strong dips at ω_2. Numerical results lead us to throw away all the arguments about experimental error or some multiphoton mechanisms that change the refractive index at ω_2 (remember that we are inside the absorption band). In the next two sections we try to present qualitative (Section 3) and quantitative (Section 4) explanations of the difference in SH response in the two cases.

3. Role of Losses at ω_2 on the Second-Harmonic Response

A more detailed look at Figs. 2–5 reveals that they are not that different, at least qualitatively: some of the dips are accompanied by small peaks, and some of the peaks are accompanied by shallow dips. This combination is quite typical for the resonance anomalies in the linear optics of diffraction gratings, and it reflects the fact that resonance anomalies that are connected with one or several poles of the scattering matrix are also accompanied by zeros of the propagating-order amplitudes. The response of the system is determined by the relative distance between the poles and the zeros from the real axis of angles of incidence and their mutual separation. This relation is discussed quantitatively in Section 4. Here we only want to point out that the differences among Figs. 2–5 can be

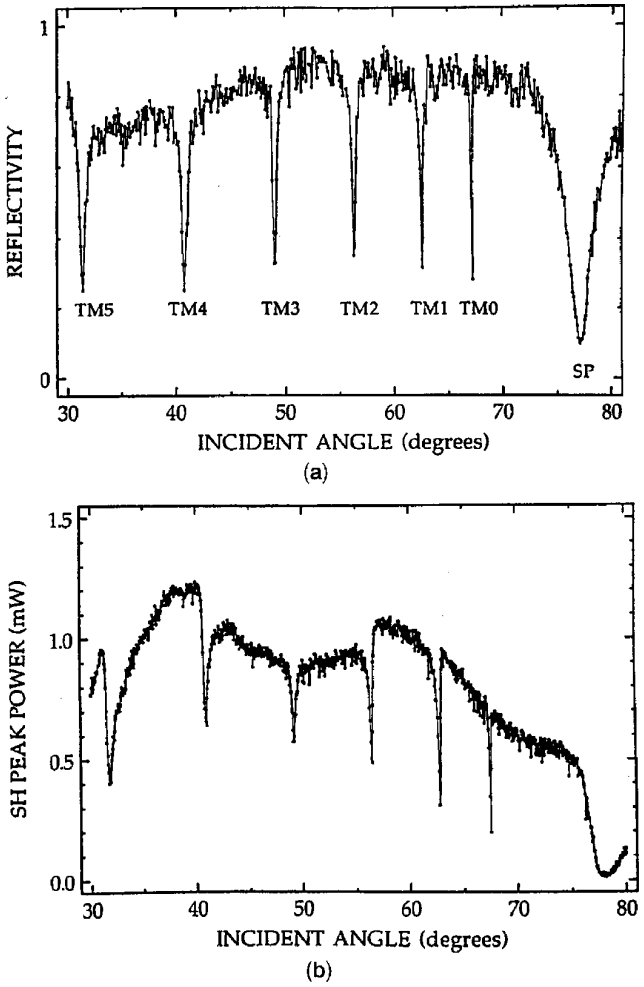

Fig. 4. (a) Experimental linear reflectivity at wavelength 1.064 μm. (See figure 5 of Ref. 7.) (b) Experimental SH peak power detected in the specular reflectance as a function of the angle of incidence. The pump wavelength is 1.064 μm, and the pump power is 2.5 MW. (See figure 6 of Ref. 9.)

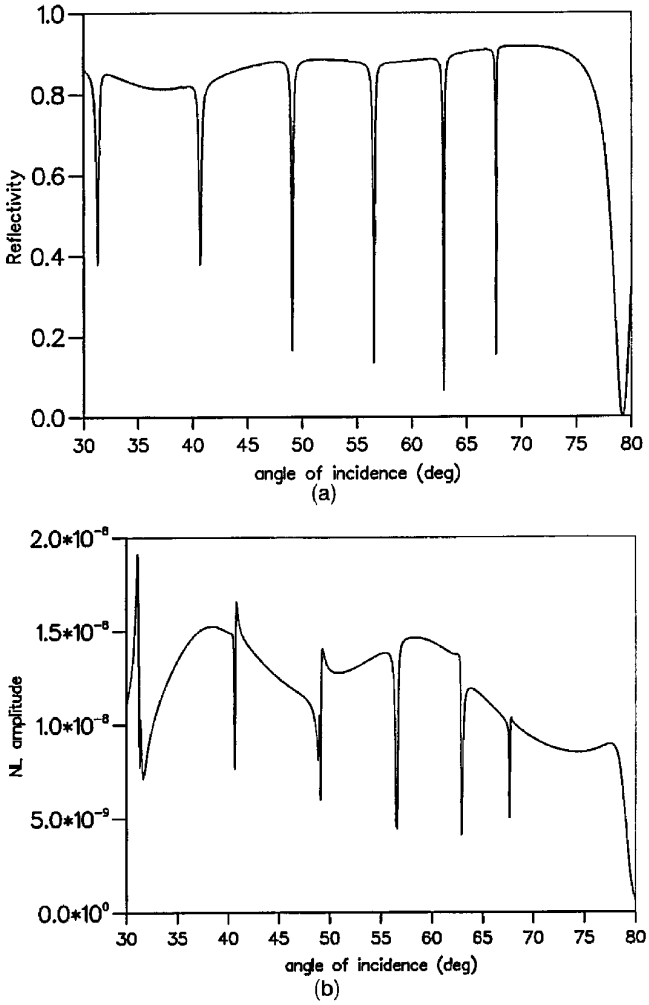

Fig. 5. Numerical angular dependence of (a) linear reflectivity and (b) NL specular order with a pump frequency of 1.064 nm. The groove period is 1.66 μm, the groove depth is 0.08 μm, and the thickness is 3.05 μm, and the polarization is TM. $n_2(\omega_1) = 1.574802 + i0.00004$, $n_3(\omega_1) = 0.13 + i7.474$, $n_2(\omega_2) = 1.6010998 + i0.0593343$, $n_3(\omega_2) = 0.051 + i3.16622$.

formulated in a simple manner: resonance anomalies are accompanied by dips and peaks of amplitudes of the propagating orders. Sometimes the dips are much more pronounced, and sometimes the peaks can be observed more easily. Let us try to analyze each case in turn to connect the differences in behavior with the losses at ω_2 inside the NL layer.

A. Pump Wavelength 1.319 μm

In this case the angular dependence of the SH generation consists of a low background with several peaks of different height [Figs. 3(b)–3(d)]. Notice that the ordinate contains the amplitude, not the efficiency, otherwise the difference between the peaks should be squared. One of these peaks (at 48.8°) is higher than the others. To find the reason for this, we have reduced the losses of the layer at ω_2, which can be easily done in computer simulations. The initial losses correspond to the experimental ones, so that the attenuation length of light inside the layer is approximately 30 μm. The linear and the NL specular responses are plotted with dashed curves. When compared with the reflectivity at ω_1, one can conclude that the peaks are due to resonance phenomena at ω_1, but not at ω_2 (mechanism I of Section 2). Reducing the losses, however, reveals that the highest peak in the angular dependence of the NL amplitude occurs when two anomalies at ω_1 and ω_2 coincide: the solid curve in Fig. 3(a) represents the linear reflectivity at ω_2, with the imaginary part of the refractive index 100 times smaller that for the dashed curve. These losses correspond to a propagation length of several millimeters. Shortening the attenuation length (dashed curves) does not considerably affect the peaks that are due to resonances only at ω_1 [Fig. 3(d)], because this attenuation length is still 10 times greater than the layer thickness. Thus, when a guided wave is excited at ω_1, the NL wave is immediately radiated in the cladding. However, if a resonance at ω_2 is also involved, as is the case with the peak at 48.8°, then the losses at ω_2 reduce the peak height by almost 2 orders of magnitude. Thus short-

ening of the propagation length from millimeters to tens of micrometers is critical in the phase-matching case.

B. Pump Wavelength 1.064 μm

In this case the double frequency falls inside the absorption band of the material of the NL layer, so that the losses at ω_2 are so high that the attenuation length becomes shorter than the layer thickness. Then the resonances at ω_1 lead to field enhancement inside the layer and thus to an enhancement of the electromagnetic field at ω_2, but this field enhancement is obtained inside a highly absorbing medium, which has a thickness comparable to the attenuation length. That is why the resonances lead to enhanced absorption instead of enhanced SH generation; i.e., dips at both ω_1 and ω_2 appear.

4. Phenomenological Approach, Nonlinear Zeros, and Quantitative Explanation of Anomalies

In the low-lossy case the role of losses in changing the NL response of the corrugated waveguide can easily be understood: The absorption losses decrease the attenuation length of the guided waves, which is responsible for the resonance. Mathematically this is reflected as an increased imaginary part of the propagation constants $p_{1,2,\ldots}$ of the guided waves. The mechanism involving only the resonance at ω_1 is not considerably affected by relatively low losses at ω_2, because the resonance response can be expressed as[10]

$$a^{\mathrm{NL}}(h) \approx a^{\mathrm{NL}}(h=0)\,\frac{c}{\left(\sin\theta_i - p_{m_1}{}^{\omega_1} + N_1\dfrac{\lambda_1}{d}\right)^2}, \quad (1)$$

where a^{NL} is the amplitude of the specular order at ω_2 for a plane interface $(h=0)$ and for the corrugated case; m_1 is the guided-wave number and N_1 is the diffraction order, which is responsible for the coupling between the incident and the guided waves. At the maximum a^{NL} is inversely proportional to $[\mathrm{Im}(p^{\omega_1})]^2$, so that the losses at ω_2 do not affect the resonant part, unless they are too high, as discussed below.

However, when a phase matching between the guided waves at ω_1 and ω_2 occurs, the NL response is determined by two resonant terms:

$$a^{\mathrm{NL}}(h) \propto \frac{c_1}{\left(\sin\theta_i - p_{m_1}{}^{\omega_1} + N_1\dfrac{\lambda_1}{d}\right)^2} \times \frac{c_2}{\left(\sin\theta_i - p_{m_2}{}^{\omega_2} + N_2\dfrac{\lambda_2}{d}\right)}. \quad (2)$$

Because the imaginary part of p^{ω_2} depends directly on the absorption losses, so does the resonant SH generation. A detailed view of the specular NL amplitude in the region of the double resonance is given in Fig. 6. Figures 6(a) and 6(b) correspond to shorter and longer propagation lengths, respectively. The propagation constants of the modes that are phase matched at incident angle 48.8° are equal to $p^{\omega_1} = (0.752578 + i0.000361)$, $p^{\omega_2} = (0.752651 + i0.002855)$ for Fig. 6(a) and $p^{\omega_2} = (0.7526515 + i0.000105)$ for Fig. 6(b). The ratio between the imaginary parts of the guided-wave propagation constants at ω_2 is approximately 28, a value corresponding quite well to the ratio between the maximum values in the two cases. As long as the imaginary part of p^{ω_2} is smaller in the second case, the resonance curve is narrower. The coefficients of proportionality c_1 and c_2 are discussed below. The flat-case NL amplitude for Fig. 6(a) is equal to 5.576×10^{-8} and for Fig. 6(b) is equal to 6.174×10^{-8}, the difference coming from the higher losses in the first case. In fact this small difference explains why the SH enhancement that concerns only resonances at ω_1 is only slightly influenced by the relatively small losses at ω_2.

These intuitive speculations, however, fail completely when applied to the high-lossy case, as presented in Figs. 4 and 5. In the previous paper[10] we

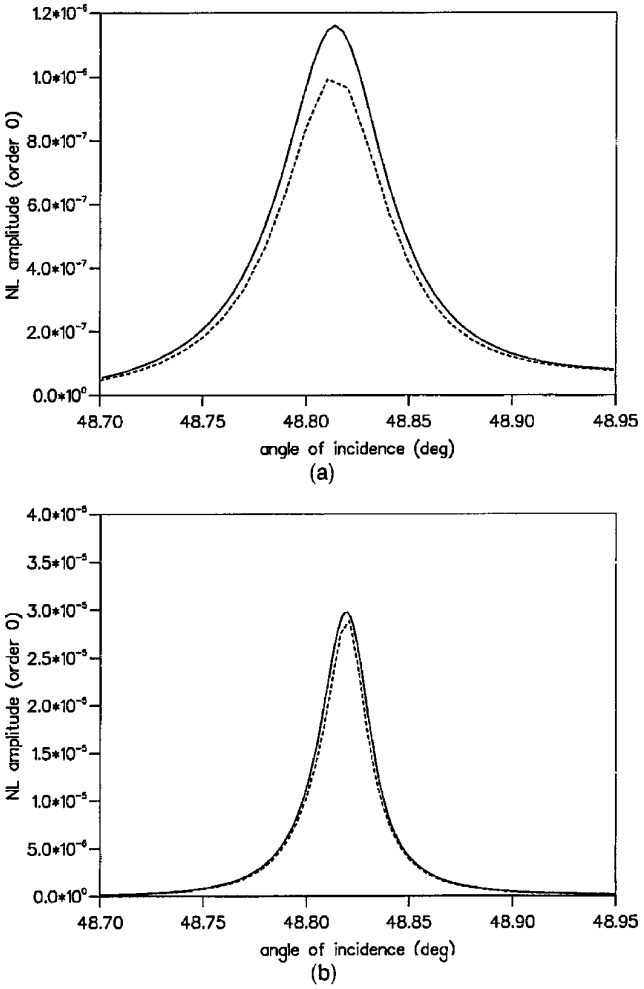

Fig. 6. (a) Enlarged view of Fig. 3(b). Dashed curve, numerical results; solid curve, phenomenological results. (b) Same as fig. 6(a) but corresponding to Fig. 3(c).

have already discussed in detail that in NL optics, similar to the linear resonance anomalies, excitation of guided waves leads to a behavior more complicated than expressed by the simple Eqs. (1) and (2). In a few words, the guided-wave excitation leads to terms such as the denominators in Eqs. (1) and (2). The values $(p - \lambda/d)$ act as poles for the scattered amplitude, so that the amplitude becomes infinite when $\sin\theta_i$ is equal to the pole(s). This is impossible for the real angle of incidence so that the peaks are limited in height. However, when the groove depth tends to zero, the grating coupling between the incident and the guided waves must vanish. Thus the poles (zeros of the denominator) must be compensated by zeros of the numerator, which tend to the poles as h tends to 0. More simple for understanding is the following argument. The NL response of the corrugated waveguide consists at least of two terms: the nonresonance response $a_{\text{flat}}^{\text{NL}}(h)$ and the resonance response $a_{\text{res}}^{\text{NL}}(h)$. The former term is close to the flat-layer NL response, and the latter is given by Eqs. (1) or (2), depending on the resonance type. Let us take the more complicated double-resonance case. Summation of the two contributions

$$a^{\text{NL}} = a_{\text{flat}}^{\text{NL}} + \frac{c}{\left(\sin\theta_i - p_{m_1}^{\omega_1} + N_1\frac{\lambda_1}{d}\right)^2\left(\sin\theta_i - p_{m_2}^{\omega_2} + N_2\frac{\lambda_2}{d}\right)} \tag{3}$$

should result in a numerator that is a third-order polynomial of $\sin\theta_i$. Thus the numerator has three zeros, z_1, z_2, and z_3, so that Eq. (3) can be rewritten as

$$a^{\text{NL}} = a_{\text{flat}}^{\text{NL}}\frac{(\sin\theta_i - z_1)(\sin\theta_i - z_2)(\sin\theta_i - z_3)}{\left(\sin\theta_i - p_{m_1}^{\omega_1} + N_1\frac{\lambda_1}{d}\right)^2\left(\sin\theta_i - p_{m_2}^{\omega_2} + N_2\frac{\lambda_2}{d}\right)}. \tag{4}$$

Of course the zeros, like the poles, are complex, but at a given nonzero groove depth they are different from the poles. Equation (4) is well known in the linear grating theory as the phenomenological formula.[16] When multimode anomalies are considered, several poles and zeros have to be included. As is obvious from Eq. (4), when the zeros are well separated from the poles, they lead to dips in the angular behavior of a^{NL} when the angle of incidence is close to their real part (minus integer time λ/d). Well separated means that the distance between the zero and the pole is greater than their imaginary parts.

And really, a detailed numerical analysis of the NL amplitude in Fig. 6 reveals that in addition to the poles, complex zeros of the amplitude can be found. For the case presented in Fig. 6(a), two of the zeros are close to the real axis, but their real parts differ (0.7535 and 0.7508) from the real parts of the poles, and they lie outside the resonance. In fact, at $\sin\theta_i = 0.7508$, which corresponds to $\theta_i = 48.66°$, a weak minimum of the amplitude can be observed [Figs. 3(b) and 3(d)]. In the other case [Fig. 6(b)] the real parts of the three zeros correspond to angles of incidence of 48.63°, 48.89°, and 48.9°, so that they lie completely outside the resonance domain. How well this approach [Eq. (4) with three zeros and three poles included] can repeat the NL response can be observed in Fig. 6, in which the solid curves represent the angular behavior, reconstructed by the use of the phenomenological formula, taking as a coefficient of proportionality the NL reflectivity of the flat system.

Believing now that it is much safer to use an equation similar to Eq. (4) for the resonance response than to rely on a simpler equation, such as Eq. (1) or (2), we can easily understand why for a very highly absorbing case instead of peaks, as expected from Eq. (1), one can observe dips (Figs. 4 and 5). Although the NL reflectivity of the noncorrugated system is only 3–4 times smaller than in Fig. 6, high absorption moves the NL zeros closer to the real axis of the angle of incidence so that the zeros play a dominant role in the angular dependency. As a typical example, the double dip that lies close to 56.5° is enhanced in Fig. 7 (dotted curve) and compared with the corresponding phenomenological curve, which was obtained from Eq. (4) with two poles (the first is a double pole) and three zeros:

$$\begin{aligned} p^{\omega_1} &= 0.834182 + i0.0007436, \\ p^{\omega_2} &= 0.836693 + i0.0651772, \\ z_1 &= 0.834719 + i0.0000539, \\ z_2 &= 0.836696 + i0.0651797, \\ z_3 &= 0.833550 - i0.0001281. \end{aligned} \tag{5}$$

The second zero almost coincides with the second pole, and their imaginary parts are much larger (because of the high losses at ω_2) than their separation, so they do not influence the reflectivity, which is a function of real angles of incidence. The first and the third zeros have real parts that correspond to

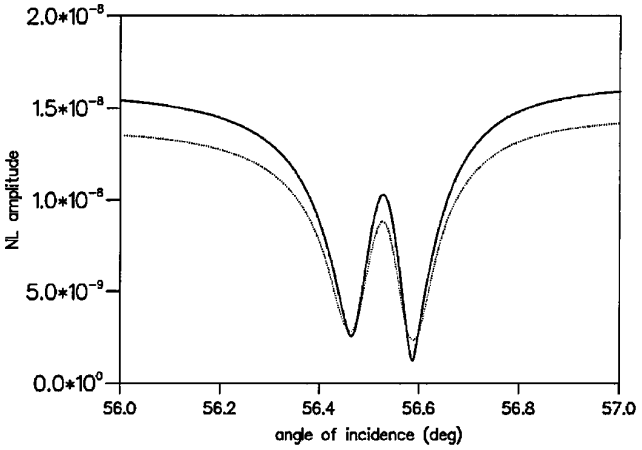

Fig. 7. Same as in Fig. 6 but corresponding to Fig. 5(b).

angles of incidence equal to 56.59° and 56.46°, respectively. Their imaginary parts are several times smaller than the imaginary parts of the remaining double pole, so that the zeros cause two dips in the NL reflectivity; the small bump between them is due to the first pole, whose real part corresponds to an angle 56.53°.

5. Phase Matching and Enhancement of Second-Harmonic Generation

We have already demonstrated that phase matching of the incident wave to the guided wave at ω_1 and to the guided wave at ω_2 can be a cause for enhancement of the NL system response. This is most obvious in Fig. 3(c), in which the only visible peak corresponds to phase matching, the effect of single resonances at ω_1 [the other three peaks in Figs. 3(b) and 3(d)] being much weaker. However, Fig. 3(c) concerns a propagation constant at ω_2 that is several millimeters, $\mathrm{Im}[n_2(\omega_2)] = 2.7 \times 10^{-5}$, whereas the experimental values are much worse, $\mathrm{Im}[n_2(\omega_2)] = 2.7 \times 10^{-3}$, and then the phase-matched peak is only 3 times higher than the others [Fig. 3(b)]. To see if it is possible to have higher enhancement, we have tried to phase match directly (without the help of the grating) the fundamental waveguide mode at ω_1 with the second waveguide mode at ω_2. Directly here stands for the fact that the parameters of the system have been chosen so that $p_1^{\omega_1} = p_2^{\omega_2}$. To couple the incident wave to the mode at ω_1, we have chosen $N_1 = 1$, expecting the strongest coupling. Then the coupling of the mode at ω_2 to the reflected NL wave is carried out through $N_2 = 2$, as far as $\lambda_1 = 2\lambda_2$. Varying the

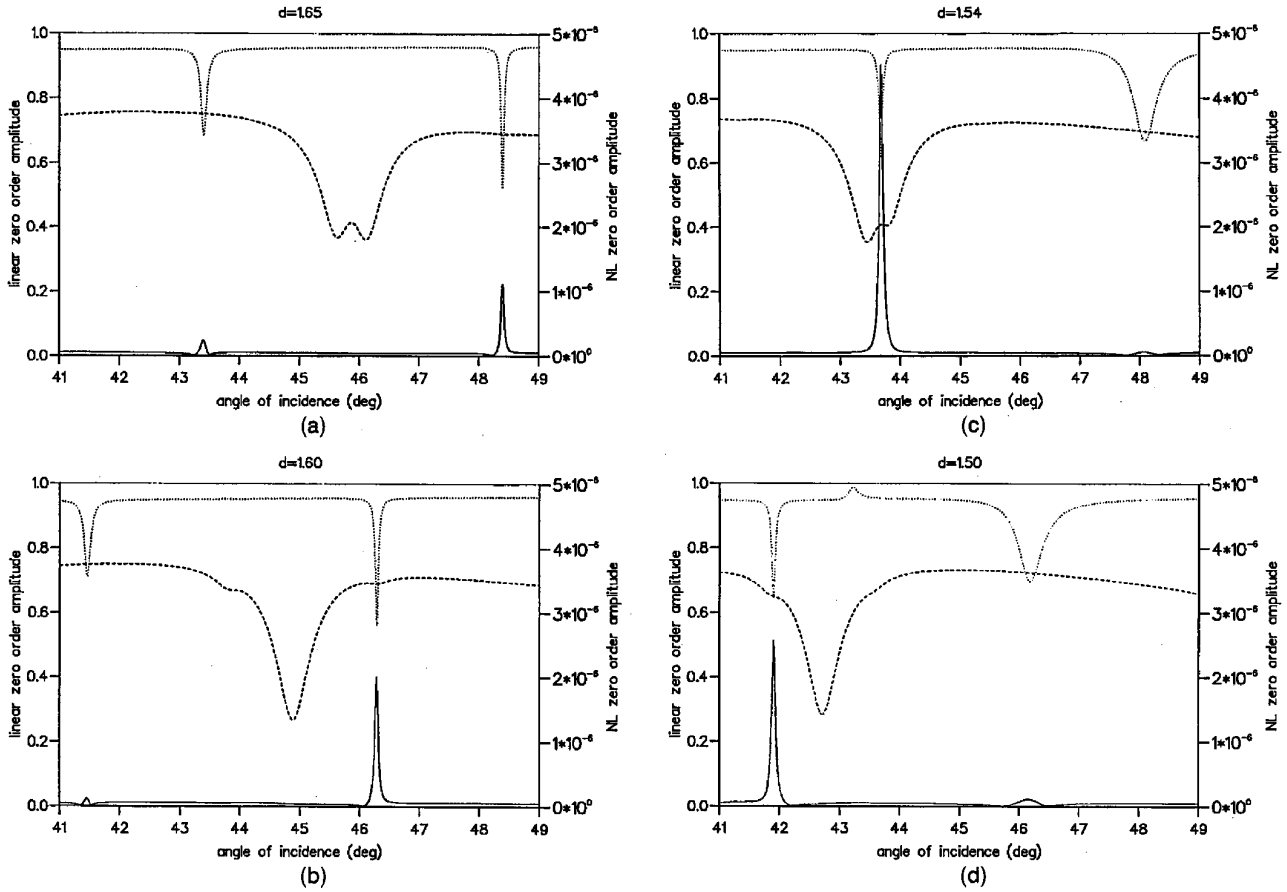

Fig. 8. Angular dependence of linear reflectivities at 1.319 mm (dotted curve) and at 0.6595 mm (dashed curve) and of the NL specular amplitude (solid curve) when the groove period d is varied. The system parameters correspond to the dashed curve in Fig. 3(a). (a) d = 1.65 μm, (b) d = 1.60 μm, (c) d = 1.54 μm, (d) d = 1.50 μm.

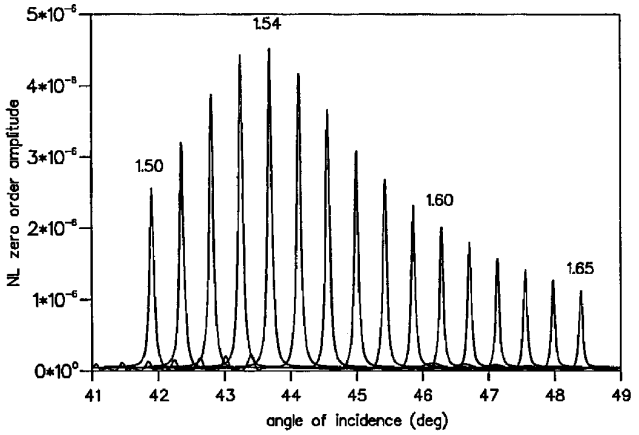

Fig. 9. NL specular amplitude for different groove periods, given in micrometer. The parameters are as in Fig. 3(b).

grating period [Figs. 8(a)–8(d)], one can observe that the anomaly of the linear reflectivity at ω_2 moves twice as slowly as the anomaly of the linear reflectivity at ω_1 (as well as the peak of the NL reflectivity). When the two anomalies coincide [Figs. 8(c) and (9), with $d = 1.54$ μm), the NL response increases almost 4 times. This should result in efficiency that is 16 times larger.

There is another anomaly at ω_1 that moves with the same speed. It corresponds to the next waveguide mode. The second anomaly at ω_2 moves with twice the speed of the first and corresponds to the ninth waveguide mode, which is excited through $N_2 = 1$. As is obvious, the effect of these anomalies on the NL reflectivity is much lower.

5. Conclusion

Inside the range of uncertainty of the optogeometric parameters, the recent electromagnetic theory of SH generation[10,15] accounts for all the complicated features observed in the experiment. Moreover, it can provide a simple explanation in a phenomenological way by showing the existence of complex poles and zeros at SH frequency. In fact the explanation is similar to the one given in linear optics[16] for total absorption of light by a bare or a dielectric-coated grating, except that in the NL case there are several poles and zeros simultaneously involved. Depending on their relative location, which is strongly influenced by the losses, an enhancement of the pump field can result either in a maximum or a minimum (or both) at the signal SH response. Thus the paper by Kull *et al.*[9] can be considered as the first experimental evidence of the existence of complex zeros of the SH amplitudes, although their existence has already been pointed out in NL optics for Kerr effect in a grating coupler.[17] These zeros are interesting not only on a fundamental level but also in view of possible applications. Because they can drastically reduce the intensity at SH frequency, the behavior of these zeros must be known when one is optimizing SH generation.

The authors acknowledge the support of the European Community through the Brite Euram contract "Flat Optical Antennas."

References

1. D. S. Chemla and J. Zyss, eds., *Nonlinear Optical Properties of Organic Molecules and Crystals* (Academic, New York. 1987), Vols. 1 and 2.
2. R. Ulrich, "Nonlinear optical organics and devices," in *Organic Materials for Nonlinear Optics*, R. A. Hann and D. Bloor, eds., Proceedings of the Conference on Applied Solid State Chemistry (Royal Society of Chemistry, London, 1988), pp. 241–263.
3. T. K. Gaylord and M. G. Moharam, "Analysis and applications of optical diffraction by gratings," Proc. IEEE **73,** 894–937 (1986).
4. G. I. Stegeman, "Introduction to nonlinear guided wave optics," in *Guided Wave Nonlinear Optics*, D. B. Ostrowsky and R. Reinisch, eds. (Kluwer, Dordrecht, The Netherlands, 1992), pp. 11–27.
5. A. D. Boardman, K. Booth, and P. Egan, "Optical guided waves, linear and nonlinear surface plasmons," in *Guided Wave Nonlinear Optics*, D. B. Ostrowsky and R. Reinisch, eds. (Kluwer, Dordrecht, The Netherlands, 1992), pp. 201–230.
6. T. Kanetake, K. Ishikawa, T. Hasegawa, T. Koda, K. Takeda, M. Hasegawa, K. Kubodera, and M. Kobayashi, "Nonlinear optical properties of highly oriented polydiacetylene evaporated films," Appl. Phys. Lett. **54,** 2287–2295 (1989).
7. J. Messier, F. Kajzar, C. Sentein, M. Barzoukaz, J. Zyss, M. Blanchard-Desce, and J. M. Lehn, "Nonlinear optical susceptibilities of asymmetric push–pull polyenes," Nonlin. Opt. **2,** 53–62 (1992).
8. F. Kajzar, "Organic molecules for guided wave quadratic and cubic optics," in *Guided Wave Nonlinear Optics*, D. B. Ostrowsky and R. Reinisch, eds. (Kluwer, Dordrecht, The Netherlands, 1992), pp. 87–111.
9. M. Kull, J. L. Coutaz, and R. Meyrueix, "Experimental results of second harmonic generation from a polyurethane waveguide on grating coupler," Opt. Lett. **16,** 1930–1932 (1991).
10. M. Neviere, E. Popov, and R. Reinisch, "Electromagnetic resonances in linear and nonlinear optics: phenomenological study of grating behavior through the poles and the zeros of the scattering operator," J. Opt. Soc. Am. B **12,** 513–523 (1995).
11. C. T. Field and F. M. Davidson, "Photorefractive two-wave mixing in the presence of high-speed optical phase modulation," Appl. Opt. **32,** 5285–5398 (1993).
12. X. H. Wang and G. K. Cambrell, "Simulation of strong nonlinear effects in optical waveguides." J. Opt. Soc. Am. B **10,** 2048–2055 (1993).
13. O. P. Nestiorkin, V. I. Safonov, and B. Ya. Zel'dovich, "Nonlinear theory of two- and four-wave interaction by means of stationary grating recorded by different-frequency waves," J. Opt. Soc. Am. B **11,** 53–60 (1994).
14. W. Samir, S. J. Garth, and C. Pask, "Interplay of grating and nonlinearity in mode coupling," J. Opt. Soc. Am. B **11,** 64–71 (1994).
15. E. Popov and M. Neviere, "Surface-enhanced second harmonic generation in nonlinear corrugated dielectrics: new theoretical approaches," J. Opt. Soc. Am. B **11,** 1555–1564 (1994).
16. M. Neviere, "The homogeneous problem," in *Electromagnetic Theory of Gratings*, R. Petit, ed. (Springer-Verlag, New York, 1980), Chap. 5.
17. R. Reinisch, M. Neviere, P. Vincent, and G. Vitrant, "Radiated diffracted orders in Kerr-type grating couplers," Opt. Commun. **91,** 51 (1992).